Effect of carrier trapping on the hysteretic current-voltage characteristics in $Ag/La_{0.7}Ca_{0.3}MnO_3/Pt$ heterostructures

D. S. Shang,[1,2] Q. Wang,[1] L. D. Chen,[1,*] R. Dong,[1,2] X. M. Li,[1] and W. Q. Zhang[1]
[1]*State Key Laboratory of High Performance Ceramics and Superfine Microstructures, Shanghai Institute of Ceramics, Chinese Academy of Sciences, Shanghai 200050, People's Republic of China*
[2]*Graduate School of the Chinese Academy of Sciences, Beijing 100039, People's Republic of China*
(Received 11 January 2006; revised manuscript received 27 March 2006; published 22 June 2006)

The current-voltage (*I-V*) characteristics and resistance switching mechanism of $Ag/La_{0.7}Ca_{0.3}MnO_3$(LCMO)/Pt sandwiched films, which were deposited on $Pt/Ti/SiO_2/Si$ substrates by pulse laser deposition, were investigated. The *I-V* characteristics can be explained by hole carrier injected space charge limited (SCL) conduction controlled by Ag/LCMO interface traps exponentially distributed in energy. The hysteresis and asymmetry in the *I-V* curves are due to trapping/detrapping process of hole carriers. The resistance changes under different voltage range are related to the carrier trapping levels induced by the positive voltage bias. Retention property of resistance is attributed to ordering/disordering transition, which is discussed on the basis of trap-assisted interface phase separation scenario. Therefore, the resistance switching induced by voltage pulses is attributed to the interface induced bulklike limited transport effect.

DOI: 10.1103/PhysRevB.73.245427 PACS number(s): 73.50.−h, 72.80.−r, 75.70.−i

I. INTRODUCTION

A. Motivation

Perovskite manganite $ReAMnO_3$ (Re=rare earth ions, A=alkaline ions), have been the subject for intense studies due to their unusual electronic and magnetic properties, such as colossal magnetoresistance (CMR) and colossal electroresistance (CER) effects.[1,2] Liu *et al.* reported that $Pr_{0.7}Ca_{0.3}MnO_3$ (PCMO) sandwiched between $YBa_2Cu_3O_7$ or Pt bottom electrode and Ag top electrode exhibited reversible, nonvolatile, electric-pulse-induced resistance (EPIR) switching at room temperature and under zero magnetic field.[3] The EPIR effect is pulse polarity dependent, namely one polarity pulse makes the resistance larger whereas the opposite polarity pulse makes the resistance smaller. The high resistance state (HRS) and the low resistance state (LRS) differ in their conductivity by as much as ten times. Similar resistance switching has also been observed in many kinds of materials, such as Cr-doped perovskite Ti and Zr oxides,[4] NiO,[5] TiO_2,[6] Cu_2S,[7] $Zn_xCd_{1-x}S$,[8] organic compound containing Cu^+ ion,[9] etc. Based on this special effect, a new application for nonvolatile memory called resistance random access memory (RRAM) have been introduced, which is very promising for its easy fabrication, fast switching speed (<100 ns), high density, and low power consuming.[10] However, the mechanism of such EPIR phenomenon is still not clear. Main disputes about this phenomenon are whether the resistance change results from bulk or the interface between the electrode and the film. Aoyama *et al.*[11] gave evidence that the resistance switching is caused by bulk properties by measuring the light reflectance of $Pr_{0.7}Ca_{0.3}MnO_3$ film, but the role of electrodes was not eliminated. Odagawa *et al.*[12] observed that the current-voltage (*I-V*) characteristics of $Ag/Pr_{0.7}Ca_{0.3}MnO_3/Pt$ heterostructures exhibit the space charge limited (SCL) current effect, and then suggest that the resistance switching induced by *I-V* hysteresis is attributed to the bulk limited conduction transition between the trap-filled SCL conduction and the trap-unfilled SCL conduction. However, Baikalov *et al.*[13] pointed out that the interfacial layer between Ag electrode and $Pr_{0.7}Ca_{0.3}MnO_3$ film is responsible for the switching, and Sawa *et al.*[14] believed that the resistance switching only occurs at $Ti/Pr_{0.7}Ca_{0.3}MnO_3$ interface after investigating the effects of several top electrodes such as SRO, Pt, Au, Ag, and Ti on the resistance switching. Oka *et al.* proposed a unique mechanism with a first order interface metal-insulator transition.[15] In order to optimize the RRAM device including device efficiency, stability, and lifetime, a better understanding of the basic EPIR principles is necessary.

The resistance value of materials is mainly determined by the process of carrier transport. Two factors deal with the current through a relatively thin semiconductor or insulator. One is the significant barrier height at the electrode/material interface (interface effect) and the other is the trapping of carriers (bulk effect). Investigating into the carrier transport modes in semiconductors and insulators would be helpful to understand the mechanism of EPIR switching effect. Recently we have reported some EPIR switching properties of $Ag/La_{0.7}Ca_{0.3}MnO_3/Pt$ heterostructures.[16] In the present paper, we studied the carrier transport mechanism of $Ag/La_{0.7}Ca_{0.3}MnO_3/Pt$ heterostructures mainly by the measurement of *I-V* characteristics. The results show that SCL conduction controlled by traps with exponential distribution in energy has a preferable conformance with the *I-V* characteristics and the traps at the Ag/LCMO interface are the dominating factor for both *I-V* hysteretic behavior and the HRS/LRS reversible switching. Retention property of the resistance is explained by the ordering/disordering transition induced by trapping/detrapping of the injected hole carriers.

B. Theory

Main modes of carrier transport in electrode-insulators (or semiconductors)-electrode sandwich system are Ohmic, space-charge-limited (SCL) conduction, thermionic emission limited conduction (TELC), Poole-Frenkel (P-F) emission,

Fowier-Nordheim (F-N) tunneling, and so on, in which Ohmic, SCL conduction and Poole-Frenkel emission are bulk dominated mechanisms while TELC and F-N tunneling are electrode/bulk interface dominated mechanisms. These modes can be distinguished via the isothermal *I-V* correlation:[17] $I \propto V$ for Ohmic; $\ln I/T^2 \propto V^{0.5}$ for TELC; $\ln I/V \propto V^{0.5}$ for P-F; $\ln I/V^2 \propto V^{-1}$ for F-N emission with T as the absolute temperature. SCL conduction with no traps can be described by Child's law[18]

$$J = \frac{9\epsilon_0 \epsilon_r \mu_p V^2}{8d^3}, \tag{1}$$

where μ_p is the hole mobility, V is the applied voltage, d is the thickness, ϵ_0 is the permittivity of free space, ϵ_r is the static dielectric constant.

For the trap-controlled SCL conduction, the *I-V* correlations will be determined by the types of distribution of traps. We consider a case of hole-only injection and note that the reverse will be equally true for electron-only injection. The distribution for the hole trap density as a function of energy level E above the edge of the valence band and distance x from the injection contact for hole carriers can be written as

$$H(E,x) = N(E)S(x), \tag{2}$$

where $N(E)$ and $S(x)$ represent, respectively, the energy and spatial distribution functions of traps. Assuming that the spatial trap distribution is uniform within the specimen from injecting electrode to collecting electrode implies that the effective thickness of the device, under space charge conditions, remains the thickness itself, and $S(x)=1$. When the traps are confined in single or multiple discrete energy levels, and the quasi-Fermi level E_p is located above the trap energy level (called shallow traps), the functional form of the SCL conduction is given by[18]

$$J = \frac{9\varepsilon_0 \varepsilon_r \mu_p V^2}{8d^3}\theta, \tag{3}$$

in which θ is described as $\theta = p/(p+p_t)$, where p is the density of free carriers and p_t is the density of trapped carriers. When the traps distributed exponentially within the forbidden energy gap, Eq. (2) becomes[19]

$$H(E) = N(E) = N_{vb}\exp\left(-\frac{E-E_{vb}}{E_t}\right), \tag{4}$$

where N_{vb} is the trap density at the valence band edge; E_t is the characteristic energy of the exponential distribution and marks the width of the exponentially distributed traps. Small values of E_t lead to trap distributions varying rapidly with energy, while large values of E_t approximate a slowly varying trap distribution. The total density of traps N_t comprising the distribution is given by evaluating $\int N(E)dE$ from the valence band edge to infinity, yielding the result $N_t = N_{vb}E_t$. Integration also reveals that over 63% of the traps lie within E_t of the valence band edge and over 99% within $5E_t$.[19] A fully analytical derivation of the *I-V* characteristics for the distribution in Eq. (4) has been developed previously.[20] It was found that at high injection currents, the filling of traps below the quasi-Fermi level results in the current being governed by the density and energy distribution of the traps. The functional form of SCL conduction is given by[20]

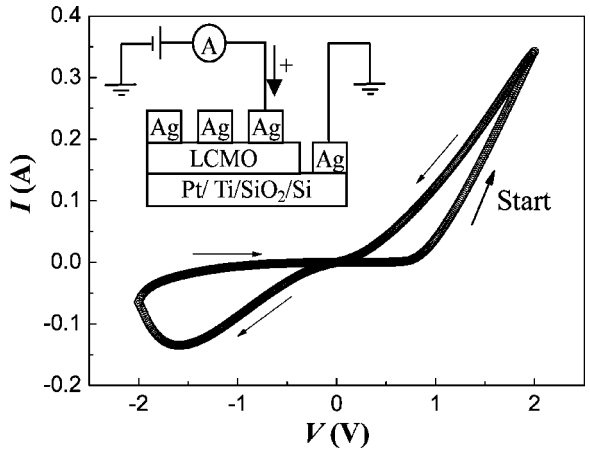

FIG. 1. *I-V* characteristic of a $Ag/La_{0.7}Ca_{0.3}MnO_3/Pt$ heterostructure at voltage sweep $0 \rightarrow -2\ V \rightarrow 0 \rightarrow +2\ V \rightarrow 0$. Arrows indicate sweeping directions. The inset shows the schematic of the samples and the measurement.

$$J = q^{1-l}\mu_p N_v \left(\frac{2l+1}{l+1}\right)^{l+1}\left(\frac{l}{l+1}\frac{\varepsilon_0\varepsilon_r}{N_t}\right)^{l}\frac{V^{l+1}}{d^{2l+1}}, \tag{5}$$

with $l = T_C/T$, where T_C is a characteristic temperature related to the trap distribution and is given by $T_C = E_t/k$, N_v is the density of the states in the valence band and k is Boltzman's constant. Upon an increase of the bias voltage, the increased positive space charge will occupy the first available trap states for holes in the band gap. That corresponds to a shift of E_p towards the valence band edge. When all the traps are filled, E_p should coincide with the valence band edge energy, namely $E_p = 0$, and the conduction mode transforms into trap free space charge limited current, which should flow obeying Child's law given by Eq. (1).

II. EXPERIMENT

$La_{0.7}Ca_{0.3}MnO_3$ (LCMO) films were grown on $Pt/Ti/SiO_2/Si$ substrates at 873 K by pulsed laser deposition technique using KrF excimer laser ($\lambda = 248$ nm) with a repetition rate of 5 Hz and a fluence of 7 J/cm^2. The deposition carried out in a pure oxygen atmosphere of the pressure of 1×10^{-2} Pa. Sintered ceramic disks of $La_{0.7}Ca_{0.3}MnO_3$ with a diameter 20 mm and thickness 5 mm were used as target material. The film thickness is about 300–800 nm controlled by deposition time. X-ray diffraction performed on the grown films indicates that the film structure is highly oriented with a (200) normal orientation. Field emission scanning electron microscopy (FE-SEM) observation indicates that the obtained films are crack-free and homogenous in composition. Electrodes of 0.5 mm diameter were contacted to the surface of LCMO film and the Pt layer respectively using Ag paint, and then heated at 473 k for 10 min. The schematic of the sandwich structure is shown in inset of Fig. 1. *I-V* curves were measured under continuous voltage sweep with 10 mV/s. The positive bias is defined by the current

flowing from the Ag top electrode to the LCMO film and then Pt bottom layer (Ag→LCMO→Pt), and the negative bias is defined by the opposite direction (Pt→LCMO →Ag). All *I-V* measurements were performed at room temperature. Usually LCMO are regarded as a *p*-type semiconductor.[21] We also measured the Hall coefficient of LCMO films on $LaAlO_3$ substrates. The results show that the LCMO films prepared in the present experiment are *p*-type materials. Therefore, the *I-V* characteristics of LCMO is mainly determined by the injection and transport of hole carriers.

III. RESULTS AND DISCUSSION

A. *I-V* measurement and space charge limited conduction mechanism

Figure 1 shows the *I-V* characteristic of a $Ag/La_{0.7}Ca_{0.3}MnO_3/Pt$ heterostructure at room temperature under the voltage sweep $0\rightarrow 2\ V\rightarrow 0\rightarrow -2\ V\rightarrow 0$. Hysteresis and asymmetry phenomena were observed clearly. It can be seen that the resistance decreased under the positive voltage sweep region and increased under the negative voltage sweep region. Two stable resistance states were obtained by the voltage sweeping.

Figures 2(a) and 2(b) show the logarithmic plots of the *I-V* curves for the positive and negative voltage sweep regions. In the $0\rightarrow +2$ V region, *I-V* curve shows linear behavior under low voltage ($<V_{on}\approx 0.18$ V), and then quadratic. At the voltage V_T (~ 0.6 V), the current rises rapidly and the slope reaches 8–10. Then, the current rises slowly and the slope reduces to 2–3. The charge transport behavior in LCMO film can be explained by one-hole carrier injected trap-controlled space charge limited (SCL) conduction mechanism. At low applied voltage, *I-V* characteristics follow Ohm's law because the density of thermally generated free carriers inside the films is predominant over the injected charge carriers. When the applied voltage reaches V_{on}, the region of *I-V* curve changes from the Ohmic to SCL conduction. In this case, the carrier transit time is equal to the Ohmic relaxation time.[18] When $V>V_{on}$, the injected excess carriers dominate the thermally generated carriers since the injected carrier transit time is too short for their charges to be relaxed by the thermally generated carriers. The conduction behavior shows that the SCL conduction is controlled by single shallow traps, which is close enough to the conduction band to be in thermal equilibrium with electrons in the conduction band. The SCL conduction with single shallow traps, given by Eq. (3), has the same square-law dependence on voltage as in the case of the trap-free SCL conduction. The SCL currents are controlled by a factor θ, the ratio of free carriers to trapped carriers. In the case of single shallow traps, the single shallow traps should be filled up at the voltage V_T (~ 0.6 V) and the current behavior should directly switch to the trap-free SCL conduction. However, in the present experiment the gradual increase (slope=8–10) in the trap-filled limit (TFL) region ($V>0.6$ V), as observed in Fig. 2(a), indicates the existence of traps distributed in trap-level energies. We assume that the trap energies have exponential

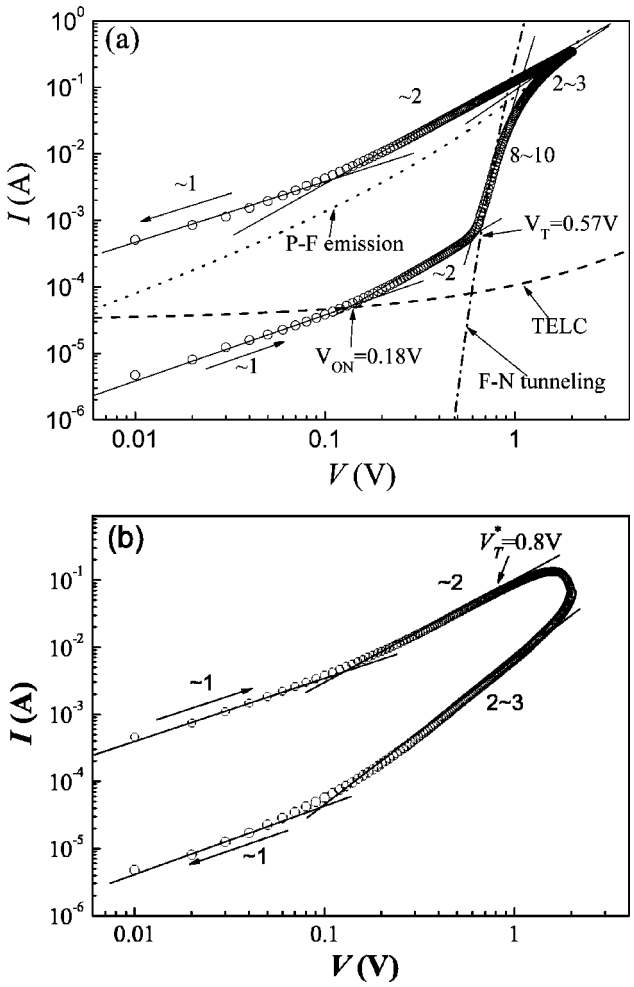

FIG. 2. *I-V* characteristics of a $Ag/La_{0.7}Ca_{0.3}MnO_3/Pt$ heterostructure in a double-logarithmic plot: (a) positive bias and (b) negative bias regions. Arrows indicate sweeping directions. The values of different slopes and V_T and V_T^* are listed in the plots. For comparison, the TELC [dashed line], P-F emission [dotted line], and F-N tunneling [dashed-dotted line] are also included in (a).

distribution in the band gap and the function is given by Eq. (4). Thus the *I-V* characteristic in the TFL region is given by Eq. (5). The slope can be used as a criterion for comparison of the stretching of the exponential distribution. Low slope implies gradual distribution, while higher slope implies abrupt distribution. The transition from the SCL conduction controlled by single shallow traps to the SCL conduction controlled by exponential distributed traps can be interpreted as follows. We deem that E_p is located above the energy level of traps E_t for hole traps initially. Thus, in the low field regime ($V<0.6$ V), the *I-V* characteristics switch from Ohmic to SCL conduction controlled by single shallow traps and follow Eq. (3). As the positive bias increases, the E_p rises toward the valence band with increasing injected electron density. At higher applied bias the E_p intersects the exponential trap distribution, and the *I-V* characteristics begin to follow Eq. (5). Moreover, if the trap distribution is deep enough, E_p may have already entered the trap distribution when the space charge limit is reached, and the *I-V* characteristics will switch directly from Ohmic to SCL conduction

with an exponential trap distribution in energy. With further increasing the applied bias, the slope in the TFL region reduces gradually, which means the existing trapping centers are gradually occupied by injected carriers, and then space charge accumulates near the electrode and creates a field impeding further injection. Thus the rate of current rise with voltage decreases and becomes constant when all traps are occupied. Trap-free space charge limited current then obeys the Child's law given by Eq. (1). In the +2 V→0 V region, *I-V* characteristics becomes linear and results in the clear hysteresis, which indicates the trapped carriers are not released completely with reducing voltage. For comparison, the TELC, P-F emission, and F-N tunneling are also shown in Fig. 2(a). The result, which is robust and does not critically depend on the values of the parameters chosen to calculate, clearly indicates that our experiment data cannot be fitted by any individual of these modes across the entire range of current. The carrier transport mechanism experiences the process of Ohmic→SCL conduction (controlled by single shallow trap)→TFL (controlled by traps with exponential distribution in energy)→SCL conduction (controlled by Child's law)→Ohmic in the region of positive voltage sweeping.

In the negative bias region, as shown in Fig. 2(b), *I-V* characteristics are similar to +2 V→0 V region before the voltage reaches $V_T^* \approx 0.8$ V. When the sweep voltage is beyond V_T^*, the current reduces with increasing voltage, which is called negative differential conductivity (NDC) phenomenon. The trapped carriers are released at V_T^* and the carrier transport mode changes from trap-free SCL conduction to SCL conduction controlled by single shallow traps. Compared V_T (~0.6 V) with V_T^* (~0.8 V), the difference between them exhibits the asymmetry between the trapping and detrapping process of hole carriers. In the voltage sweep region of −2V→0 V, *I-V* characteristics transit from SCL conduction controlled by single shallow traps to Ohmic conduction. The carrier transport mechanism in the negative voltage sweep region can be described as Ohmic→SCL conduction (controlled by Child's law)→SCL conduction (controlled by single shallow traps)→Ohmic.

B. Influences of sweep voltages and resistance states on the *I-V* hysteresis

I-V hysteresis behaviors were also examined by measuring *I-V* curves at different sweep ranges. In Figs. 3(a) and 3(b) we can see that at low value of V_{max}, *I-V* curves show the transition from Ohmic to SCL conduction controlled by single shallow traps in positive bias region but no hysteresis, which indicates the trapped carriers can be released by traps with the removing of bias at this stage, and then the resistance change is unretentive. With raising V_{max}, *I-V* curves show TFL conduction (controlled by traps with exponential distribution in energy) in the positive sweep region, meanwhile the hysteresis can be observed, which indicates the injected carriers trapped with exponential distribution in energy remain after removing the positive bias until a negative voltage of V_T^* is applied. As the V_{max} rises to 2 V, *I-V* curves show the gradual transition from TFL to trap-free SCL conduction, where the hysteresis and resistance change approach to be saturated. The above results indicate that the appearance of hysteresis depends on the carrier trapping levels. As the positive bias increased, the trapping level increases with increasing injected carrier density and the quasi-Fermi level E_p shifts towards the valence band. Only when the E_p intersects the exponential trap distribution with the increasing bias, do the retention of trapped carrier takes effect, leading to the *I-V* hysteresis and asymmetry of Ag/LCMO/Pt heterostructures.

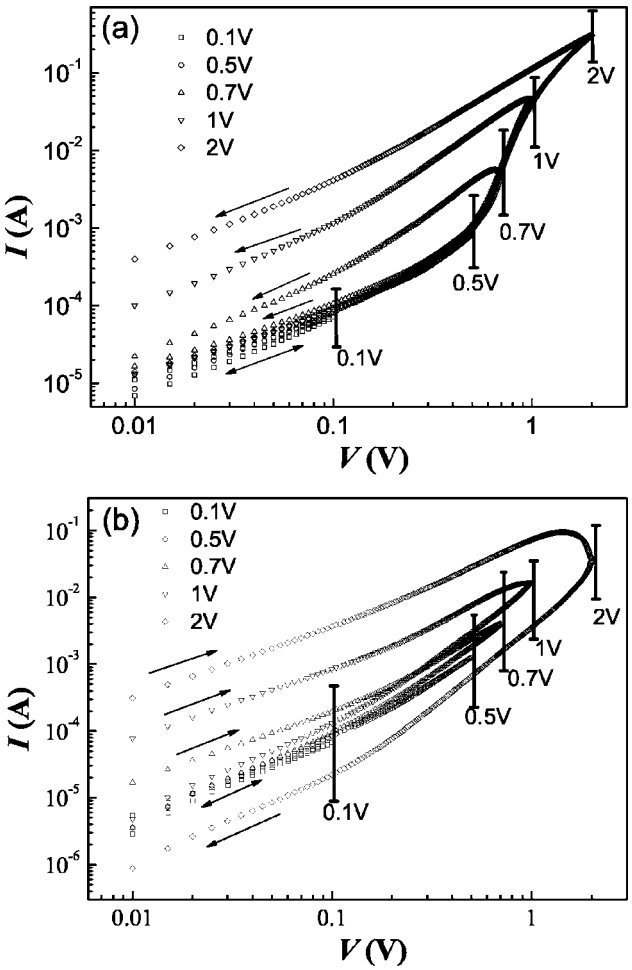

FIG. 3. *I-V* characteristics of a Ag/$La_{0.7}Ca_{0.3}MnO_3$/Pt heterostructure measured at different range of voltage sweep: (a) positive bias and (b) negative bias regions. Bias voltage swept as 0 V →V_{max}→0 V→−V_{max}→0 V with V_{max} varied as 0.1, 0.5, 0.7, 1, and 2 V. The values of different V_{max} are listed in the plots. Arrows indicate sweeping directions.

I-V characteristics of two resistance states, HRS and LRS induced by positive and negative voltage pulse (width =100 ns) respectively, were examined. In Fig. 4, *I-V* curves show Ohmic→SCL conduction (controlled by single shallow traps)→TFL (controlled by traps with exponential distribution in energy)→SCL conduction (controlled by Child's law) behaviors in HRS and Ohmic→TFL (controlled by traps with exponential distribution in energy)→SCL conduction (controlled by Child's law) behaviors in LRS, respectively. Moreover, the slope of LRS in TFL region is lower than that

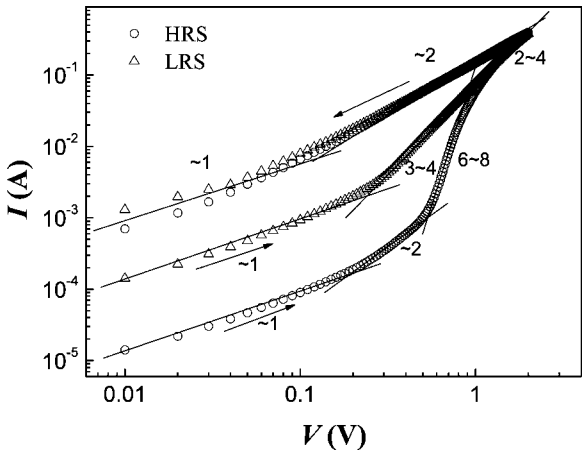

FIG. 4. *I-V* characteristics for the LRS and HRS, which were obtained by applying positive and negative voltage pulses (width =100 ns), respectively. Arrows indicate voltage sweeping directions.

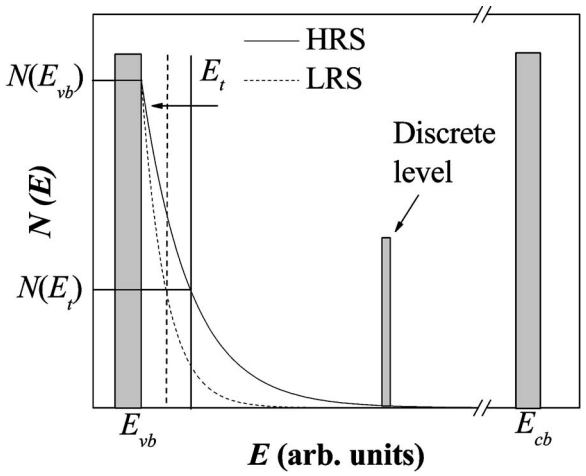

FIG. 5. Schematic diagram of the exponentially distributed density of states as a function of energy, $N(E)$, at constant temperature. E_{vb} and E_{cb} mark the edges of the valence and conduction bands, respectively. E_t is the characteristic constant of the distribution, in which the $N(E_t)$ has been reduced by $1/e$ as compared to the $N(E_{vb})$. In the band gap, the area under the exponential distribution curve indicates the total trap density. The retention property of trapped carriers causes the reduction of the total trap density and the shift of E_t towards E_{vb} in the switching from HRS to LRS.

in HRS. The slope in the TFL region can be described as Eq. (5). The decrease of TFL slope can be ascribed to the decreasing of E_t at constant temperature. We suggest that the trapping of carriers takes place and makes the quasi-Fermi level E_p shift towards the valence band in HRS→LRS process induced by voltage pulses. When the trapping level reaches the situation in which E_p intersects the exponential trap distribution (TFL region), the trapped carriers exhibits the retention property. The total number of traps in the films decreases and the exponential distribution is changed to be narrow. Thus, E_t, marking the width of the trap distribution, shifts to a new place towards the valence band edge, as shown in Fig. 5. According to the above analysis, we can conclude that the resistance switching induced by voltage pulse originates from the change of trap distribution in energy in the films and belongs to bulk limited transport effect. The resistance states are dependent on the carrier trapping levels in the films, namely the high trapping level corresponding to LRS while the low one corresponding to HRS.

C. Discussion about the interface effect and retention behavior

The measured resistance value along the vertical direction of the film (about 1–30 kΩ) is much larger than that calculated using the values of either LCMO thin film or polycrystalline ceramic (0.01–0.2 Ωcm).[22] This deviation reminds us of the effect of electrode/film interfaces resistance, especially Schottky barriers. On the basis of the rule of metal/semiconductor contact, the hole barriers should be formed at Ag/LCMO interfaces due to the different work function values of Pt (~5.3 eV), Ag (~4.3 eV), and LCMO (~4.8 eV).[17,23] However, the SCL conduction feature of *I-V* curves show that the contact of Ag/LCMO is Ohmic. Furthermore, no appreciable asymmetry with the *I-V* polarity within ±0.5 V was observed in Fig. 4, so the role of Schottky barriers should be minor, even if it exists at all. We believe that a high resistive region containing high density of defects exists at the Ag/LCMO interface, where the high density of surface states induced by the defects may cause a large degree of band bending and then influence the validity of the metal/semiconductor contact rule in our Ag/LCMO/Pt heterostructure. The high resistive region may stem from the Ag_xO/LCMO interface due to the oxygen diffusion from the LCMO film into the Ag electrode, thus leaving a thin oxygen depleted LCMO layer at the Ag/LCMO interface.[24] In the oxygen depleted layer, large oxygen vacancies are positively charge and, hence, act as donor-type native defects, increasing the resistance of the interface region because of the compensation effect.[25] The dense interface defects act as trap centers of carriers and dominate the *I-V* characteristics and EPIR properties. However, the bulk limited SCL conduction mode of the carriers is not be influenced (Fig. 2). This is consistent with the work of de Boer *et al.*,[26] in which *I-V* characteristics still show the bulklike feature of SCL conduction even in the surface trap dominated condition. Therefore, we attribute the SCL conduction in Ag/LCMO/Pt heterostructures to the interface induced bulklike limited conduction because the dominate traps are located at the Ag/LCMO interface.

Traditional one carrier injected trap-controlled SCL conduction does not, however, explain the retention behavior of trapped carriers after the applied bias is removed. The escape frequency ν of trapped carriers is given by[12]

$$\nu = \nu_0 \exp\left(-\frac{(E_t - T\Delta S)}{kT}\right), \tag{6}$$

where ν_0 is the attempt-to-escape frequency and ΔS the change in entropy required to effect an escape from a trap of depth E_t. Thus, the negative value of ΔS and the deep level of E_t increase the residence time of carriers in the traps. The

negative value of ΔS indicates the structure of system have the trend of ordering. We assume that some structure ordering around the traps took place when the traps were filled by carriers and the stability of the structure ordering can be reinforced with the enhancement of the trapping level. Since the structure ordering, the negative ΔS causes the residence time of a carrier in trap ν^{-1} increasing and the resistance change remaining. This structure ordering should be polarity dependent. Under a particular negative bias of $|V_T^*| > |V_T|$, the structure ordering is damaged. In this state, the trapped carriers are released and the resistance state is restored.

This structure ordering may be concerned with the special properties of perovskite manganites. The phase separation scenario seems a universal feature in CMR manganites.[27] The application of various external perturbations, such as magnetic field and electric current and/or field, to the multiphase systems may disturb the phase coexistence topology.[2,28] One may consider a state of equilibrium in which ferromagnetic metallic (FMM) clusters embedded in a charge-ordering insulator (COI) matrix at the region of LCMO film close to the Ag/LCMO interface. Applying the positive bias causes injected hole carriers to be trapped by the metal/insulator domain interfaces, moving the interface to the insulate side and enlarging the metallic domains.[29] In the lower trapping level state, however, the formed FMM domains is small and unstable, corresponding to the voltage sweep with $V_{max} < 0.6$ V in Fig. 3. That means the existence of a distribution of energy barriers through which the FMM phase grows against the COI phase. The energy barrier depending on the FMM fraction is one of the main factors determining the phase separation characteristics.[30] With increasing the trapping level, the formed FMM domains become larger and more stable. Then, after the system is driven to a "close-to-equilibrium state" as reported by Levy *et al.*,[31] the process cannot be reversed and the system keeps the memory of its FMM fraction after the applied bias is removed. Larger FMM domains with better connectivity would trigger a percolation process, inducing the reduction of resistance. The transition from the COI to FMM can be considered as a first-order transition,[2,32] which produces a negative ΔS according to the thermodynamics theory. Therefore, the above percolation process is a electronic structure ordering process, making the residence time of a hole carrier in trap ν^{-1} increase and the percolation state (namely the resistance state) remain after the applied bias is removed. The hole carriers are injected from Ag electrode under the positive bias and accumulated at the Ag/LCMO interface region, hence, the general metallic percolation direction is from Ag/LCMO interface to Pt/LCMO interface. Under the negative bias ($V > V_T^*$), more hole carriers are extracted from the Ag electrode than are injected from the Pt electrode, leading to the FMM region reduced. Thus the percolation state is damaged and the resistance is restored. The difference of V_T and V_T^* indicates the asymmetric barriers exist in electronic structure ordering/disordering transition, which might be due to strong interaction between large injection and the phase separation state. So the *I-V* hysterisis and EPIR switching with memory effect is manifestation of the trap-assisted interface phase separation stimulated by carrier injection. To well understand the nature and modulation process of the carrier injection on the coexistent multiphase, more detailed studies are still needed.

IV. CONCLUSIONS

We have investigated the hysteretic *I-V* characteristics of Ag/LCMO/Pt heterostructures. SCL conduction controlled by Ag/LCMO interface traps with exponential distribution in energy is employed to describe the carrier transport process. The hysteresis is observed when the carrier trapping level comes to the situation in which the *I-V* curves show the TFL conduction mechanism, and can be attributed to retention property of trapped carriers. The high and low resistance states induced by voltage pulses are also dependent on the carrier trapping levels and the resistance switching can be regarded as the changes of trap level distribution caused by trapping/detrapping process of hole carriers. This SCL conduction is attributed to interface induced bulklike limited effect because the traps dominating the carrier transport are located at the Ag/LCMO interface. Carriers filled traps with exponential distribution in energy show the nonvolatile property, which cannot be explained by traditional SCL conduction. The nonvolatility is related to the ordering/disordering transition caused by the trap-assist interface phase separation process of perovskite manganite films. The present results suggest that the resistance switching of electrode-insulator (or semiconductor)-electrode sandwich system could be dominated by the defects at the electrode/insulator (or semiconductor) interface. Improved RRAM devices can be expected by designing the interface to create a metallic/insulator phase coexistence layer where the conductivity depends strongly on the carrier injection.

ACKNOWLEDGMENTS

This work was supported in part by the National Natural Science Foundation of China under Grant Nos. 50202016 and 50325208.

*Corresponding author, Tel.: +86-21-52412520; Fax: +86-21-52413122. Electronic mail address: cld@mail.sic.ac.cn

[1] S. Jin, T. H. Tiefel, M. McCormack, R. A. Fastnacht, R. Ramesh, and L. H. Chen, Science **264**, 413 (1994).

[2] A. Asamitsu, Y. Tomioka, H. Kuwahara, and Y. Tokura, Nature (London) **388**, 50 (1997).

[3] S. Q. Liu, N. J. Wu, and A. Ignatiev, Appl. Phys. Lett. **76**, 2479 (2000).

[4] A. Beck, J. G. Bednorz, Ch. Gerber, C. Rossel, and D. Widmer, Appl. Phys. Lett. **77**, 139 (2000); Y. Watanabe, J. G. Bednorz, A. Bietsch, Ch. Gerber, D. Widmer, A. Beck, and S. J. Wind, *ibid.* **78**, 3738 (2001).

[5] S. Seo, M. J. Lee, D. H. Seo, E. J. Jeoung, D. -S. Suh, Y. S. Joung, I. K. Yoo, I. R. Hwang, S. H. Kim, I. S. Byun, J. -S. Choi, and B. H. Park, Appl. Phys. Lett. **85**, 5655 (2004).
[6] C. Rohde, B. J. Choi, D. S. Jeong, S. Choi, J. S. Zhao, and C. S. Hwang, Appl. Phys. Lett. **86**, 262907 (2005).
[7] T. Sakamaoto, H. Sunamura, H. Kawaura, T. Hasegawa, T. Nakayama, and M. Aono, Appl. Phys. Lett. **82**, 3032 (2003).
[8] P. Van der Sluis, Appl. Phys. Lett. **82**, 4089 (2003).
[9] L. Ma, Q. Xu, and Y. Yang, Appl. Phys. Lett. **84**, 4908 (2004).
[10] M. J. Rozenberg, I. H. Inoue, and M. J. Sánchez, Phys. Rev. Lett. **92**, 178302 (2004), and references therein.
[11] K. Aoyama, K. Waku, A. Asanuma, Y. Uesu, and T. Katsufuji, Appl. Phys. Lett. **85**, 1208 (2004).
[12] A. Odagawa, H. Sato, I. H. Inoue, H. Akoh, M. Kawasaki, Y. Tokura, T. Kanno, and H. Adachi, Phys. Rev. B **70**, 224403 (2004).
[13] A. Baikalov, Y. Q. Wang, B. Shen, B. Lorenz, S. Tsui, Y. Y. Sun, and Y. Y. Xue, Appl. Phys. Lett. **83**, 957 (2003); S. Tsui, A. Baikalov, J. Cmaidalka, Y. Y. Sun, Y. Q. Wang, Y. Y. Xue, C. W. Chu, L. Chen, and A. J. Jacobson, *ibid.* **85**, 317 (2004).
[14] A. Sawa, T. Fujii, M. Kawasaki, and Y. Tokura, Appl. Phys. Lett. **85**, 4073 (2004).
[15] T. Oka and N. Nagaosa, Phys. Rev. Lett. **95**, 266403 (2005).
[16] R. Dong, Q. Wang, L. D. Chen, T. L. Chen, and X. M. Li, Appl. Phys. A: Mater. Sci. Process. **80**, 13 (2005); R. Dong, Q. Wang, L. D. Chen, D. S. Shang, T. L. Chen, X. M. Li, and W. Q. Zhang, Appl. Phys. Lett. **86**, 172107 (2005).
[17] S. M. Sze, *Physica of Semiconductor Devices* (Wiley, New York, 1981).
[18] K. C. Kao and W. Hwang, *Electrical Transport in Solids* (Pergamon, Oxford, 1981).
[19] R. D. Gould and M. S. Rahman, J. Phys. D **14**, 79 (1981).
[20] P. Mark and W. Helfrich, J. Appl. Phys. **33**, 205 (1965).
[21] S. Mathews, R. Ramesh, T. Venkatesan, and J. Benedetto, Science **276**, 238 (1997); C. Mitra, P. Raychaudhuri, G. Köbernik, K. -H. Müller, L. Schultz, and R. Pinto, Appl. Phys. Lett. **79**, 2408 (2001); C. Mitra, P. Raychaudhuri, K. Dörr, K. H. Müller, L. Schultz, P. M. Oppeneer, and S. Wirth, Phys. Rev. Lett. **90**, 017202 (2003); H. Tanaka, J. Zhang, and T. Kawai, Phys. Rev. Lett. **88**, 027204 (2002).
[22] E. Dagotto, T. Hotta, and A. Moreo, Phys. Rep. **344**, 1 (2001); J. M. D. Coey, M. Viret, L. Ranno, and K. Ounadjela, Phys. Rev. Lett. **75**, 3910 (1995).
[23] D. W. Reagor, S. Y. Lee, Y. Li, and Q. X. Jia, J. Appl. Phys. **95**, 7971 (2004).
[24] A. Plecenikk, K. Frohlich, J. P. Espinos, J. P. Holgado, A. Halabica, M. Pripko, and A. Gilabert, Appl. Phys. Lett. **81**, 859 (2002).
[25] N. A. Tulina, S. A. Zver'kov, A. Arsenov, Y. M. Mukovski, and D. A. Shulyatev, Physica C **385**, 563 (2003).
[26] R. W. I. de Boer and A. F. Morpurgo, Phys. Rev. B **72**, 073207 (2005).
[27] A. Moreo, S. Yunoki, and E. Dagotto, Science **283**, 2034 (2000); M. Uehara, S. Mori, C. H. Chen, and S. -W. Cheong, Nature (London) **399**, 560 (1999); M. Fäth, S. Freisem, A. A. Menovsky, Y. Tomioka, J. Aarts, and J. A. Mydosh, Science **285**, 540 (1999).
[28] V. Markovich, E. S. Vlakhov, Y. Yuzhelevskii, B. Blagoev, K. A. Nenkov, and G. Gorodetsky, Phys. Rev. B **72**, 134414 (2005); F. X. Hu, J. Gao, and X. S. Wu, Phys. Rev. B **72**, 064428 (2005); Y. G. Zhao, Y. H. Wang, G. M. Zhang, B. Zhang, X. P. Zhang, C. X. Yang, P. L. Lang, M. H. Zhu, and P. C. Guan, Appl. Phys. Lett. **86**, 122502 (2005).
[29] T. Wu, S. B. Ogale, J. E. Garrison, B. Nagaraj, A. Biswas, Z. Chen, R. L. Greene, R. Ramesh, T. Venkatesan, and A. J. Millis, Phys. Rev. Lett. **86**, 5998 (2001).
[30] L. Ghivelder and F. Parisi, Phys. Rev. B **71**, 184425 (2005).
[31] P. Levy, F. Parisi, L. Granja, E. Indelicato, and G. Polla, Phys. Rev. Lett. **89**, 137001 (2002).
[32] A. Masuno, T. Terashima, Y. Shimakawa, and M. Takano, Appl. Phys. Lett. **85**, 6194 (2004).